# Spin dependence of the giant-dipole-resonance strength function in highly excited nuclei in the mass region $A = 39-45$

M. Kicińska-Habior
*Institute of Experimental Physics, University of Warsaw, 00681 Warsaw, Poland and Nuclear Physics Laboratory, University of Washington, Seattle, Washington 98195*

K. A. Snover, J. A. Behr, G. Feldman,* C. A. Gossett, and J. H. Gundlach
*Nuclear Physics Laboratory, University of Washington, Seattle, Washington 98195*
(Received 11 October 1989)

Continuum $\gamma$-ray spectra and angular distributions from decays of highly excited $^{39}$K, $^{40}$K, $^{42}$Ca, and $^{45}$Sc compound nuclei produced by bombarding $^{27}$Al with $^{12}$C, $^{13}$C, $^{15}$N, and $^{18}$O ions have been measured and the giant-dipole-resonance strength function has been extracted. The effective temperature associated with the states upon which the giant dipole resonance is built is nearly constant (1.7–1.8 MeV) for these reactions, while the final average spin varies from 8 to 18.5$\hbar$ as the projectile energy varies from 32 to 72.5 MeV. The parameters of the giant-dipole-resonance strength function extracted from fits of statistical model calculations to the $\gamma$-ray spectra measured at $\theta_\gamma = 90°$ provide direct information on the spin dependence of the hot nuclear shape. The mean energy of the giant dipole resonance shows a weak spin dependence that has a different character for $^{39}$K and $^{45}$Sc nuclei. The width of the giant dipole resonance increases rapidly with spin for all reactions studied, from 11.6±0.3 MeV at 8$\hbar$ to 14.7±0.5 MeV at 18.5$\hbar$ for $^{45}$Sc* at $T_f = 1.7-1.8$ MeV, for example, presumably due to rotational broadening of the giant dipole resonance. For the reactions $^{12}$C+$^{27}$Al at $E_{lab} = 62.7$ MeV and $^{18}$O+$^{27}$Al at $E_{lab} = 44.9$ and 72.5 MeV, angular distributions have been measured. The observed energy dependence of the $a_2$ coefficient suggests large nuclear deformation consistent with oblate noncollective or prolate collective rotation. The level density in nuclei with $A \cong 40$ has been calculated in the Reisdorf approach with parameters fitted to low-energy level density data for nuclei in this mass region.

## I. INTRODUCTION

During recent years much work has been done experimentally on investigating the giant dipole resonance (GDR) built on highly excited states of compound nuclear systems produced in heavy-ion collisions.[1–16] Most of these studies concern medium- and heavy-mass nuclei, while very little information on the GDR in equilibrated light nuclei is available.[12] In a study of the temperature and spin dependence of the GDR strength function in the statistical GDR decay of $^{63}$Cu* (Ref. 14), the energy and strength of the GDR were found to be independent of spin and temperature, while the width of the GDR was found to increase as a function of both temperature and spin. In that work as well as in a similar study for heavier nuclei[11] both the effective temperature and the spin of the final state upon which the GDR is built increase with increasing bombarding energy and hence their influence on the GDR strength function cannot be separated.

In this paper we examine the GDR strength function in $^{39}$K, $^{40}$K, $^{42}$Ca, and $^{45}$Sc nuclei at elevated temperature, in order to investigate possible spin-induced nuclear shape changes. These nuclei are nearly spherical in their ground states, except for $^{45}$Sc which has a slightly prolate shape.[17] However, at higher spin, an oblate deformation with rotation around the symmetry axis is predicted for nuclei with $A \simeq 40$.[18–20] Very little experimental information concerning this effect is known.

We formed the compound nuclei of interest at moderate, nearly constant, effective temperature and over a large range of spin in heavy-ion fusion reactions using an aluminum target and $^{12}$C, $^{13}$C, $^{15}$N, and $^{18}$O projectiles. For these nearly mass-symmetric reactions, an increase in the projectile bombarding energy increases both the compound nuclear excitation energy and the rotational energy by nearly the same amount. The difference of these energies (diminished by the dipole vibration energy) determines the effective temperature of the final states upon which the GDR is built (see Sec. III C). Hence, the effective temperatures are nearly constant for these reactions (see Table I), while the angular momentum varies as a function of bombarding energy. Thus, we are able to study the spin dependence of the GDR strength function, hence the nuclear shape, at constant temperature. For the cases studied, the initial excitation $E_{xi}$ varies from 40.0 to 66.6 MeV and the grazing angular momentum $l_0$ changes from 11.5 to 28$\hbar$, corresponding to an average initial spin $I_i = 2l_0/3 = 8-18.5\hbar$. The effective temperatures for most cases are in the range of $T_f = 1.7-1.8$ MeV.

The parameters of the GDR strength function were extracted from fits of the statistical model calculations to the measured $\gamma$-ray spectra at $\theta_\gamma = 90°$. In order to test

 

TABLE I. Characteristics of the compound nuclear states populated in the present work.

| Compound nucleus | Entrance channel | $E_{lab}$[a] (MeV) | $l_0$ ($\hbar$) | $E_{xi}$ (MeV) | $T_f$[b] (MeV) |
|---|---|---|---|---|---|
| $^{39}$K | $^{12}$C+$^{27}$Al | 62.7 | 24.7 | 60.0 | 1.69 |
| | | 48.2 | 19.8 | 50.0 | 1.71 |
| | | 33.8 | 11.5 | 40.0 | 1.75 |
| $^{40}$K | $^{13}$C+$^{27}$Al | 39.7 | 14.0 | 46.3 | 1.88 |
| $^{42}$Ca | $^{15}$N+$^{27}$Al | 44.7 | 18.7 | 50.2 | 1.78 |
| | | 29.2 | 11.5 | 40.2 | 1.77 |
| $^{45}$Sc | $^{18}$O+$^{27}$Al | 72.5 | 28.0 | 66.6 | 1.78 |
| | | 61.5 | 24.4 | 60.0 | 1.77 |
| | | 44.9 | 19.8 | 50.0 | 1.73 |
| | | 31.5 | 11.5 | 42.0 | 1.69 |

[a]$E_{lab}$ averaged over the target thickness.
[b]Estimated as in Ref. 14 based on CASCADE statistical model calculations, and using $a = A/8$ MeV$^{-1}$.

the assumption of statistical decay in the heavy-ion fusion reactions presently studied and also to improve our understanding of the role of deformation in compound nuclei formed at high excitation, we have measured angular distributions of $\gamma$ rays from the decays of $^{39}$K* at $E_{xi}=60.0$ MeV and $^{45}$Sc* at $E_{xi}=50.0$ and 66.6 MeV. For statistical emission of high-energy $\gamma$ rays, the angular distribution in the center of mass must be symmetric about $\theta_\gamma=90°$. The existence of an asymmetry would be an indication of a nonstatistical reaction process.[10]

For purely statistical decay of a spherical nucleus, the angular distribution in the center of mass is expected to be nearly isotropic. If, however, the compound system possesses a definite deformation, a $\gamma$-decay anisotropy (which is symmetric about 90°) is expected (Ref. 21, see also, Ref. 10). The anisotropy depends on the type of deformation (oblate or prolate) and on the orientation of the deformed shape with respect to the rotational axis. For pure dipole decay this results in a nonzero $a_2$, the coefficient of the Legendre polynomial $P_2(\cos\theta)$. Experimental evidence for this effect has been found previously in the decay of Er* isotopes.[22,23]

Our measured angular distributions are symmetric about $\theta_\gamma=90°$ for $E_\gamma > 10$ MeV, confirming the statistical nature of the $\gamma$-emission process in the GDR region. Nonzero $a_2$ coefficients are observed, consistent with oblate noncollective or prolate collective rotation. Deformation averaging calculations reproduce the observed $a_2$ coefficients in the high-energy region and indicate preferred deformations $\beta \geq 0.15$ at the highest bombarding energy, consistent with the oblate deformation expected in the rotating liquid-drop model.

The treatment of the level density is of particular concern in statistical GDR decay analysis. We present a consistent analysis of the $\gamma$-ray spectra from the decay of four different initial compound nuclei with $A \cong 40$ which allows us to choose between different level density formulations. Data which provide direct information on the level density at the high energies relevant to statistical GDR decay are either scarce or nonexistent. Extrapolation of the level density upward from lower energies where data exist is difficult because these energies span the range where shell and pairing corrections to the nuclear mass are expected to disappear, and the rate of their disappearance, which is uncertain, must be properly taken into account. Among the level density formulations currently available, the damping of shell effects is best handled in the Reisdorf approach[24] which we describe in Sec. III B 1. However, the Reisdorf level density parameters are not suitable for light nuclei, and we present a determination of suitable parameters. We also discuss the Pühlhofer approach,[25] which is commonly used because it is built into the CASCADE computer code.

## II. EXPERIMENTAL DETAILS

Self-supporting rolled aluminum targets of 99.999% chemical purity and 1.0 and 1.5 mg/cm$^2$ thickness were bombarded with $^{12}$C, $^{13}$C, $^{15}$N, and $^{18}$O ions from the University of Washington FN tandem Van de Graaff accelerator. Gamma rays from the decay of the compound nuclei studied were detected in a 25.4 cm×25.4 cm NaI(Tl) detector surrounded by a plastic anticoincidence shield. Our experimental technique was very similar to that described previously.[14]

In order to check for the presence of light impurities, particularly oxygen and carbon, in the aluminum targets, additional measurements were performed using a $^{12}$C beam at $E_{lab}=17$ MeV, which is above the Coulomb barrier for reactions on carbon and oxygen target nuclei but below the Coulomb barrier for aluminum. The amount of light impurities in the $^{27}$Al targets was estimated to be $<1\%$, and these impurities made a negligible contribution to the spectra of interest.

For all cases studied, the $\gamma$-ray yield was measured at $\theta_\gamma=90°$ with respect to the beam axis. For three cases, $^{18}$O+$^{27}$Al at $E_{lab}=44.9$ and 72.5 MeV and $^{12}$C+$^{27}$Al at $E_{lab}=62.7$ MeV, additional measurements were performed with the NaI spectrometer positioned at angles $\theta_\gamma=40°$, 60°, 90°, 120°, and 140°. Due to the significant yield of high-energy neutrons, especially at forward angles, all data were taken in event mode (pulsed-beam time

of flight and $\gamma$-ray energy recorded) and sorted off-line. For the angular distribution data, varying time gates based on a series of 1-MeV wide $\gamma$-ray energy bins were used in order to account for a small slewing in the time signal from the gamma detector. During the experiment, special care was taken to avoid systematic errors which would influence the data differently at different angles. Pileup was suppressed using an electronic rejection circuit. An additional correction was made in software to account for the fact that the rejection circuit was not 100% efficient. All data were taken with a constant counting rate of 15 kHz (above 0.25 MeV) in order to minimize pileup differences at different angles, and several sweeps through the full set of angles were made at each bombarding energy in order to check internal consistency.

All absolute cross sections were obtained by direct calculation from the measured $\gamma$-ray yields, after correcting for pileup and deadtime as described in Ref. 14.

## III. RESULTS

The measured $\gamma$-ray spectra at $\theta_\gamma = 90°$ produced by the decay of the compound nuclei $^{39}$K*, $^{40}$K*, $^{42}$Ca*, and $^{45}$Sc* formed at different initial excitation energies and initials spins are presented in Fig. 1. The cross-section scale was derived assuming isotropic angular distributions. The solid curves represent statistical model calculations which are described below.

### A. Statistical model analysis

Gamma-ray cross sections were calculated using a modified version of the computer code [25]CASCADE including the effect of isospin.[12] The parameters of the GDR (peak energy $E_D$, width $\Gamma$, and strength $S$ in units of the classical dipole sum rule) were treated as variables in the least-squares fitting of the calculated spectra to the experimental data. The fitting region was $E_\gamma \geq 12$ MeV, the region where the spectrum shape is most sensitive to the GDR parameters. Isoscalar (ISGQR) and isovector (IVGQR) giant quadrupole resonances have been included in the calculations with fixed parameters based on ground-state systematics.[26,27] The $E2$ contributions were small ($<7\%$ for $E_\gamma < 20$ MeV, $\sim 10\%$ for $E_\gamma = 25$ MeV), and the calculated spectrum shapes were insensitive to changes of GQR parameters.

Although the CASCADE calculations including the effect of isospin are much more time consuming then those with the normal isospin-independent version of the code, they were necessary because of the large importance of isospin for these light nuclei. We found that the fits done with and without including the effects of isospin were not simply related by a strength renormalization factor as is the case for heavier masses.[14] Isospin affects not only the strength by relatively large factors of 1.3–1.8 but also the extracted values of $E_D$ and $\Gamma$ by up to 5 and 7 %, respectively, for the present cases. Hence, all the fits presented here were done including the effects of isospin. We neglected possible isospin mixing, which, in somewhat lighter nuclei, was found to be small.[12]

Fusion cross sections for $^{12}$C+$^{27}$Al (Ref. 28), $^{15}$N+$^{27}$Al (Ref. 29), and $^{18}$O+$^{27}$Al (Refs. 30 and 31) reactions are known experimentally. For projectile energies $E_{lab} = 50$ MeV and above, the fusion cross sections calculated with CASCADE are within 10% of the experimental values. For lower energies, discrepancies up to 25% occur between calculated and experimental values. In our analysis we used CASCADE default fusion cross sections for energies $E_{lab} \geq 50$ MeV. For lower projectile energies, the calculated spectra have been normalized to agree at low $\gamma$-ray energy with the measured spectra by varying the grazing angular momentum $l_0$. Fusion cross sections determined in this manner together with experimentally measured values are presented in Table II.

### B. Level density

As in our previous paper,[14] we have examined the suitability of the level density formulation given by Pühlhofer,[25] together with variations, and the Reisdorf approach.[24] The Reisdorf approach is much more sensible, in principle, and with parameters fitted to low-energy level density data, it results in good fits to all the $\gamma$-ray spectra from the GDR decay. Here the level density at all excitation energies is given by one smoothly varying formula in which the parameter $a$ is dependent on the ground-state shell correction energy and the excitation energy of the nucleus.

The Pühlhofer approach, on the other hand, is not as good a method, in principle, and in nuclei presently studied ($A \cong 40$) can be made to work only with somewhat arbitrary and uncertain parameter adjustments which are different for neighboring nuclei. The basic problem with the Pühlhofer approach is that the low-energy ($E_x \leq 10$ MeV) and high-energy ($E_x \geq 20$ MeV) regions are treated independently. The level density in the high-energy region is not tied to experimental data, nor may it be extrapolated to sufficiently low energy, in most cases neutron threshold, where data do exist. As a result, in the region of interpolation between low and high energies, the slope of the level density is commonly wrong, and this affects the shape of the calculated $\gamma$-ray spectrum and the extracted GDR parameters. Nevertheless, with parameter adjustment one can achieve a reasonable level density for many nuclei with this approach.[14] However, care has to be taken to check the smoothness of the level density curve and to compare it with existing experimental data.

Below we present an analysis of the level density for nuclei with mass $A = 23-120$. Our goal was to reproduce the level density for nuclei with mass $A \cong 40$. Our calculated level densities were compared with available experimental data, which consists of level density values determined from direct level counting, high-resolution $s$- and $p$-wave neutron resonance and charged-particle resonance measurements, one-nucleon transfer reactions, and fluctuation analyses.[32,33] These data cover the range mainly up to $\sim 10$ MeV; for some nuclei the level densities up to $\sim 25$ MeV are known. We then performed CASCADE calculations for decays of $^{39}$K*, $^{40}$K*, $^{42}$Ca*, and $^{45}$Sc* nuclei using level densities based on this

analysis. Some additional background information is given in our previous paper.[14]

### *1. The Reisdorf approach*

Here we discuss our attempt to reproduce the level density for nuclei with mass $A \cong 40$ with the Reisdorf approach.[14,24] In this approach the level density is given by

$$\rho(E,I)=\frac{2I+1}{12\theta^{3/2}}\sqrt{a}\,\frac{\exp(2\sqrt{aU})}{U^2} \quad (1)$$

with

$$aU=\tilde{a}\{U+\delta U[1-\exp(-\gamma U)]\}\ , \quad (2)$$

where $U=E-I(I+1)/\theta+\delta P$, $I$ is the angular momentum, and $\theta=2J/\hbar^2$ is the moment of inertia parameter. The damping parameter $\gamma^{-1}$ and the level density parameter $\tilde{a}$ are described below. The shell plus pairing correction to the ground-state mass is given by the difference of the experimental mass $M_{\rm exp}$ and the calculated liquid-drop mass $M_{\rm LD}$ such that $\delta U+\delta P=M_{\rm exp}-M_{\rm LD}$. Equation (2) applies to energies $U$ which are sufficiently high that the pairing correction to the level density are assumed to have vanished; hence the appearance of the

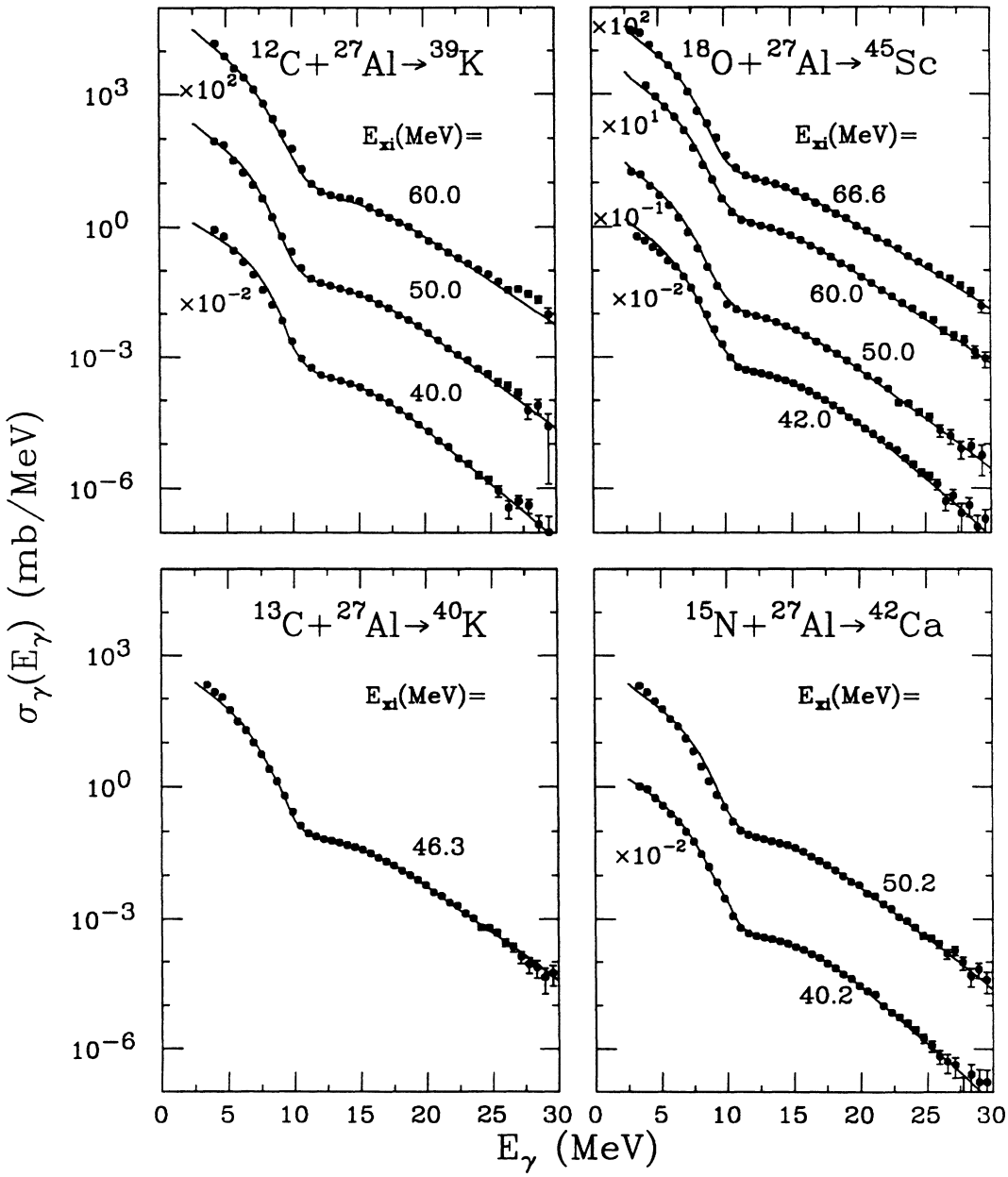


FIG. 1. Measured $\gamma$-ray spectra at $\theta=90°$ from the decays of $^{39}K^*$, $^{40}K^*$, $^{42}Ca^*$, and $^{45}Sc^*$ together with least-squares-fitted statistical model calculations using the level density calculated in the Reisdorf approach with the odd-$A$ pairing reference, $\gamma^{-1}=18.5$ MeV and $r_0=1.10$ fm.

TABLE II. Fusion cross sections used in CASCADE calculations.

| Entrance channel | $E_{lab}$ (MeV) | $\sigma_{fusion}$ (mb) Present work[a] | Previous work | Ref. |
|---|---|---|---|---|
| $^{12}C+^{27}Al$ | 62.7 | 1144 | 1140±170 | 28 |
| | 48.2 | 967 | 1045±160 | 28 |
| | 33.8 | 524 | ~600[b] | 28 |
| $^{13}C+^{27}Al$ | 39.7 | 592 | | |
| $^{15}N+^{27}Al$ | 44.7 | 860 | 930±120 | 29 |
| | 29.2 | 561 | 600±80 | 29 |
| $^{18}O+^{27}Al$ | 72.5 | 1131 | 1220±38 | 31 |
| | 61.5 | 1015 | 1150±35 | 31 |
| | 44.9 | 922 | 880±30 | 31 |
| | 31.5 | 499 | 418±17 | 30 |

[a]For $E_{lab} > 50$ MeV, this is the default value from CASCADE. For $E_{lab} < 50$ MeV, this value was determined from a fit to the low-energy part of the $\gamma$-ray spectrum.
[b]Extrapolated from higher energy.

"backshift" factor $\delta P$. At low energies where pairing is important, the factor $\delta P$ should be absent. We treat the behavior at low energies in an approximate manner by extrapolating Eqs. (1) and (2) down to $E \cong 3-5$ MeV, below which the level density is given by the counting of individual levels. The shell correction factor $\delta U$ is assumed to be damped more slowly than $\delta P$ with excitation energy, hence it appears in Eq. (2) multiplied by the damping factor $1-\exp(-\gamma U)$.

The pairing corrections $\delta P$ are calculated in a standard way using the droplet model of Myers.[34] Originally in the droplet model the odd-$A$ pairing reference was used, in which the pairing correction equals zero for odd-$A$ nuclei.[34] However, Reisdorf[24] used the even-even reference, while Schmidt in the microscopic calculations of the level density[35] recommended the odd-odd reference. The ground-state shell corrections $\delta U$ are determined by $\delta U = M_{exp} - M_{LD} - \delta P$. Thus, both pairing and shell corrections depend on the choice of the pairing reference, and hence the deduced level density depends on the reference. It is not obvious which of the pairing references should be used.[36] In this work we used the odd-$A$ reference, with $\delta P = \pm 11 A^{-1/2}$ (MeV) and zero. Some calculations have been done in all three references and the sensitivity of the extracted GDR parameters has been tested using level densities determined from different pairing references.

The parameter $\tilde{a}$, which is assumed to be independent of energy and to vary smoothly with mass, is calculated according to a microscopic description[24] containing surface and curvature corrections

$$\tilde{a} = 0.04543 r_0^3 A + 0.1246 r_0^2 A^{2/3} B_S + 0.1523 r_0 A^{1/3} B_K \ , \quad (3)$$

where the parameters $r_0$, $B_S$, and $B_K$ are defined in the droplet model of Myers.[34] The numerical coefficients in Eq. (3) are taken from the HIVAP computer code,[37] and are somewhat different for the surface and curvature terms than the values given in Ref. 24. Our calculations have been done using the level density subroutine from HIVAP, which we have incorporated into CASCADE. We assume[24] $B_S = B_K = 1$ and we concentrate on the parameter $r_0$ which should be very close to the nuclear matter radius constant.[38] In the original Reisdorf approach,[24] $r_0$ was treated as a free parameter together with $\gamma^{-1}$ and $p = \delta P A^{1/2}$ in a fitting procedure of the experimental neutron resonance spacings for nuclei with $A = 100-253$. The best-fit parameters were $r_0 = 1.153 \pm 0.01$ fm, $\gamma^{-1} = 18.5$ MeV, and $p = 10.5 \pm 2$. Although the level density calculated in this manner with these parameters works well for $A \cong 63$,[14] it does not work well, in general, for other light nuclei. In the mass region of $A \cong 40$ the level density calculated with these parameters and the odd-$A$ pairing reference is 2–5 times larger than the experimental values.[32,33] This is shown in Fig. 2, where the total level density $\rho(E)$ (summed over allowed spins), calculated with the Reisdorf parameters and the odd-$A$ pairing reference is shown by dashed lines for some nuclei with $A = 35-45$ and compared with experimental data.[32,33] A similar discrepancy between calculated and experimental densities is shown in Fig. 3(a), which displays ratios of the level spacings calculated with the Reisdorf parameters to the experimental level spacings[32,33] for nuclei with mass $A = 23-65$ at particular spins and at particular excitation energies in the range $5 \text{ MeV} \le E_x \le 12$ MeV. A similar effect is observed when the even-even reference is used. With the odd-odd reference, the agreement between the calculated and experimental level spacings is better in the mass region $A \cong 40$, but it is much worse for heavier masses, as shown in Fig. 4.

The question then arises as to whether the parameters $\gamma^{-1}$ and $r_0$ should be independent of $A$. To test the sensitivity of the level density to changes in $\gamma^{-1}$ and $r_0$ we have varied the parameter $\gamma^{-1}$ from 6 to 25 MeV and $r_0$ from 1.153 to 1.10 fm, for the three pairing references and nuclei with mass $A = 23-65$. We found that decreasing $\gamma^{-1}$ worsens the discrepancy between experimental and calculated values beyond that shown in Fig. 4, whereas increasing $\gamma^{-1}$ above the Reisdorf value of 18.5 MeV makes only a slight improvement, independent of the pairing reference. On the other hand, the common expectation that the damping of shell effects should scale with temperature (as opposed to excitation energy $U$) implies that $\gamma^{-1}$ should be smaller in lighter nuclei. Since we do not have a good justification for increasing $\gamma^{-1}$, we decided to leave it fixed at 18.5 MeV.

The calculated level density is, however, very sensitive to changes in $r_0$ since $r_0$ appears to the third power in the parameter $\tilde{a}$ [Eq. (3)]. In the case of the odd-$A$ and even-even pairing references, reducing $r_0$ below 1.153 fm improves the agreement between calculated and experimental level densities for $A \cong 40$. We found that to reproduce the level density for nuclei in the mass range $A = 35-45$, the best values of $r_0$ are the same for the odd-$A$ and even-even references, namely 1.10 fm, while for the odd-odd reference $r_0 = 1.153$ fm is the best. The

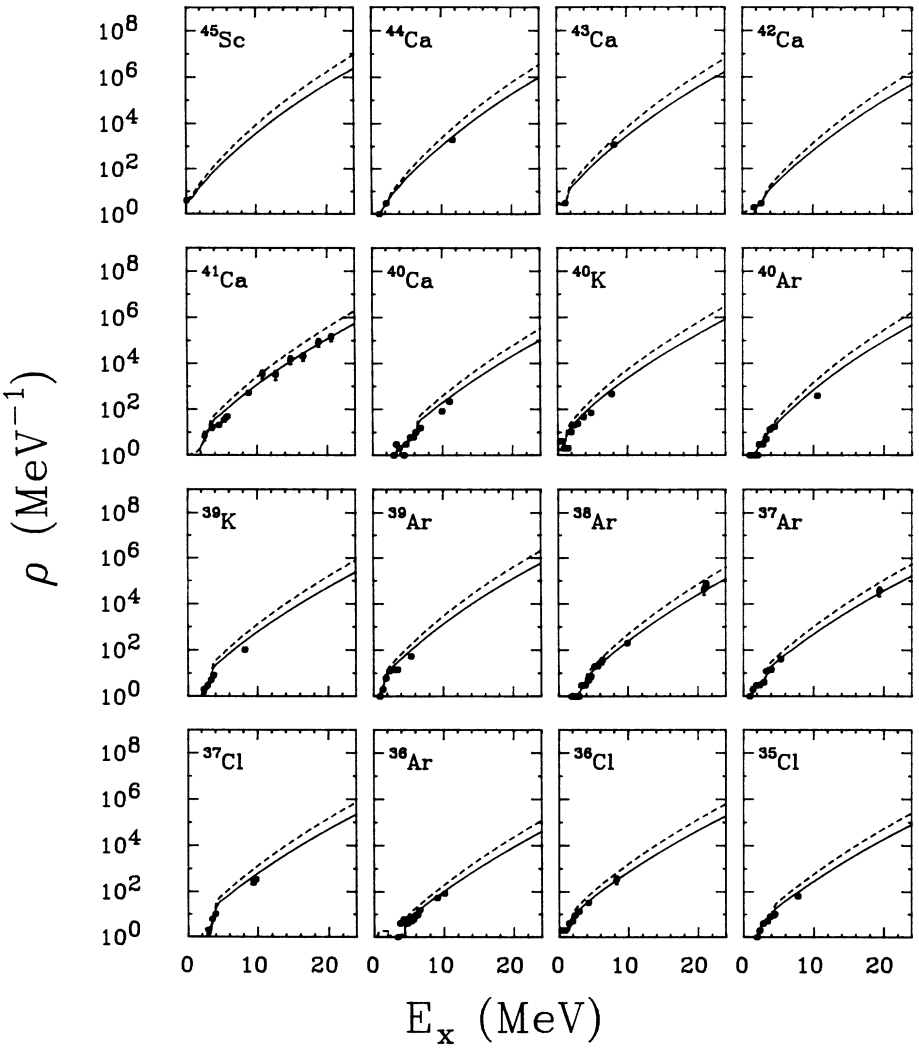


FIG. 2. Total level density curves for some nuclei important in the decay of $^{39}$K*, $^{40}$K*, $^{42}$Ca*, and $^{45}$Sc* together with the experimental data (solid points) from Refs. 32 and 33. Level densities are calculated in the Reisdorf approach with the odd-$A$ pairing reference, $\gamma^{-1}=18.5$ MeV, and two values of $r_0$: 1.153 fm (dashes) and 1.10 fm (solid lines).

total level density curves calculated with parameters $\gamma^{-1}=18.5$ MeV and $r_0=1.10$ fm in the odd-$A$ reference presented by solid lines in Fig. 2 reproduce the experimental data[32,33] much better than those with $r_0=1.153$ (dashes). Ratios of the level spacings calculated with these best parameters to the experimental level spacings[32,33] are presented for the odd-$A$ reference in Fig. 3(b) for comparison with those calculated with the Reisdorf parameters [Fig. 3(a)]. In Fig. 5 these ratios, calculated with the best parameters for each of the three references, are shown. Even with the best parameters, discrepancies up to a factor of 2 between calculated and experimental values of the level spacing occur for some nuclei with mass $\cong 40$. This suggests that some of the shell corrections in this mass range are not correct. In Fig. 6 we show the energy dependence of the total level density calculated for $^{45}$Sc using the three different references with the best values of $\gamma^{-1}$ and $r_0$. These three level density curves have different slopes, and this affects the fitted GDR parameters, as discussed below.

Reducing $r_0$ to 1.10 fm improves the agreement between experimental and calculated level densities for $A\cong 40$, but worsens it for heavier nuclei. However, $r_0$ should be weakly mass dependent. This is illustrated in Fig. 7 which shows the equivalent sharp radius parameter $r_{0z}$ of the charge distribution for nuclei with mass $A=20-120$ obtained from the equivalent rms radius $Q_z$ in a manner similar to Ref. 38:

$$Q_z \cong r_{0z} A^{1/3}[1+\tfrac{5}{2}(b/r_{0z})^2 A^{-2/3}] . \quad (4)$$

The equivalent rms radius $Q_z=\sqrt{5/3}\langle r^2\rangle^{1/2}$ and the sur-

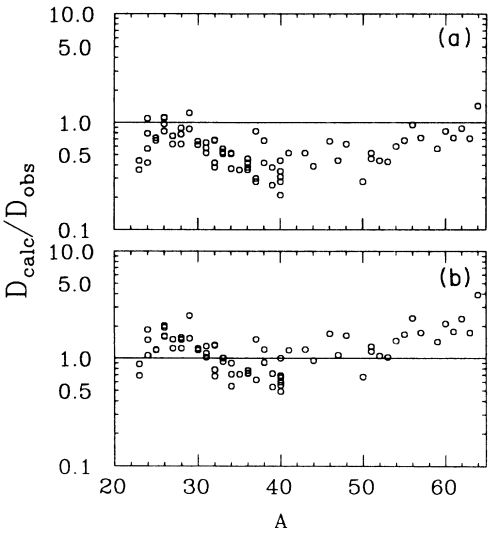


FIG. 3. Ratio of the calculated and experimental (Refs. 32 and 33) values of the level spacing for nuclei with $A=23-65$. Level spacings were calculated in the Reisdorf approach with the odd-$A$ pairing reference, $\gamma^{-1}=18.5$ MeV and the two values of (a) $r_0=1.153$ fm and (b) 1.10 fm.

face width $b=(\pi/\sqrt{3})z$ of the proton Fermi distribution have been determined from the electron scattering data for which the two-parameter Fermi model was applied.[39] Shown also in Fig. 7 is $r_{0z}$ calculated by Myers (see Fig. 5

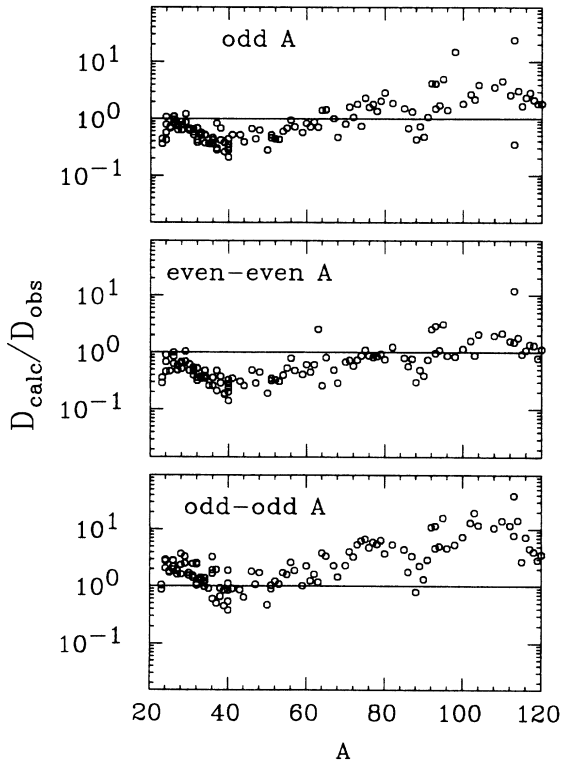


FIG. 4. The same as Fig. 3(a), but calculated level spacings obtained in the Reisdorf approach with $\gamma^{-1}=18.5$ MeV and $r_0=1.153$ fm for three pairing references and nuclei with $A=23-120$.

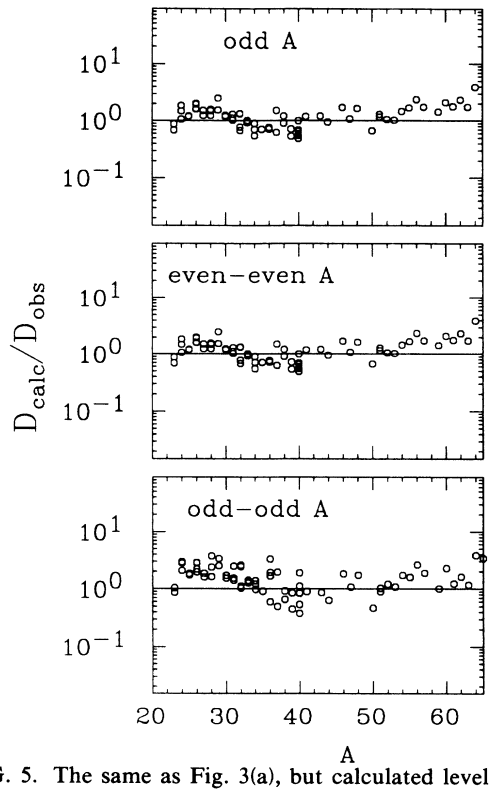


FIG. 5. The same as Fig. 3(a), but calculated level spacings obtained in the Reisdorf approach with the best parameters $r_0$ and $\gamma^{-1}$ for each of the three pairing references for nuclei with $A=23-65$ (see text).

in Ref. 40) including effects[41] due to finite nuclear compressibility, which lead to a greater squeezing of light nuclei by surface tension forces, and dilation of heavy nuclei by the electrostatic repulsion. For $A\cong 40$,

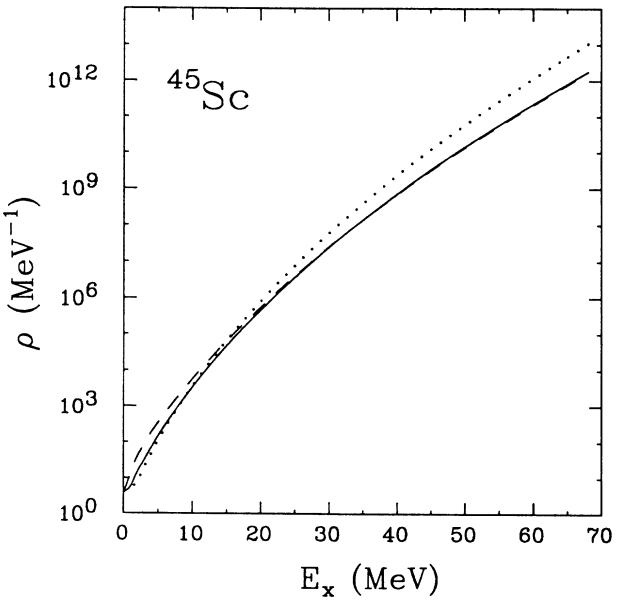


FIG. 6. Level density curves for $^{45}$Sc nucleus calculated in the Reisdorf approach with the best parameters for each of the three pairing references: the odd-$A$ reference, solid line; even-even reference, dashes; odd-odd reference, dots.

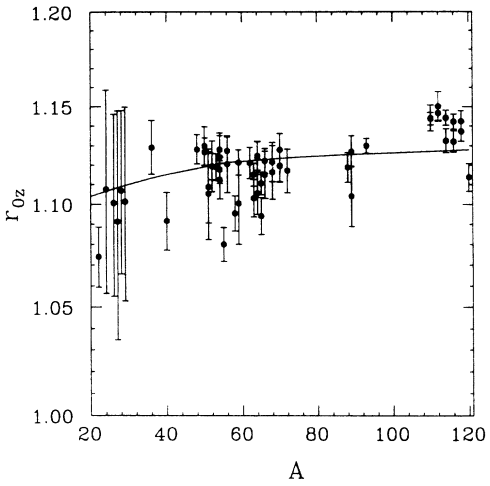


FIG. 7. Equivalent sharp radius parameter $r_{0z}$ of the charge distributions for nuclei with mass $A=20-120$. Experimental values obtained from Ref. 39 by direct calculation according to Ref. 38 (see text). The curve represents the droplet model calculation of Myers (Ref. 40).

$r_{0z}(\text{exp}) \cong 1.09$ fm, which lies somewhat below the Myers calculations (see Fig. 7). This value, together with the droplet model prediction for the difference between rms radii of the neutron and proton distribution,[42] yields $r_0 \cong 1.10$ fm, in excellent agreement with our estimate from the neutron threshold level density comparisons. Furthermore, at the substantially higher energies of 10–25 MeV, the level density calculated in the Reisdorf approach with $r_0=1.10$ fm, $\gamma^{-1}=18.5$ MeV and the odd-$A$ reference agrees with experimental values determined from fluctuation analyses (see Fig. 2). These independent studies provide confidence that the present level density formulation is sensible and reasonable.

All measured $\gamma$-ray spectra have been fitted with CASCADE calculations using $r_0=1.10$ fm and $\gamma^{-1}=18.5$ MeV, and the odd-$A$ pairing reference. With these parameters, $\tilde{a}$ lies in the range $A/8.37$ MeV$^{-1}$ to $A/8.61$ MeV$^{-1}$ for $A=39-45$. The moment of inertia parameter in the level density was approximated as spin independent. This approximation was tested by comparing to one-shot CASCADE calculations which included a spin-dependent liquid-drop moment of inertia, which showed negligible differences. From these fits the GDR parameters discussed in Sec. III C have been extracted.

In order to check the sensitivity of the GDR parameters to the choice of the level density parameters $r_0$ and $\gamma^{-1}$ as well as to the choice of the pairing reference, several fits were performed to the presently analyzed $\gamma$-ray spectra with various parameters $\gamma^{-1}$ and $r_0$ and the different references. Conservative systematic errors due to estimated level density parameter uncertainties $\Delta r_0=\pm 0.02$ fm, $\Delta\gamma^{-1}=\pm 6$ MeV, and change of pairing reference (odd-$A$, even-even, and odd-odd) are $\Delta S \cong \pm 15\%$, $\Delta E_D \cong 0.05$ MeV, $\Delta\Gamma \cong \pm 1$ MeV. We have included in $\Delta S$ a $\pm 7-12\%$ uncertainty in the fusion cross section. As discussed below, these uncertainties do not apply to the differences in GDR parameters as a function of spin, for which the relative uncertainties are much smaller. Variations of the GDR parameters with the change of pairing reference depend weakly on the excitation energy of the decaying nucleus, since the slope of the level density depends weakly on the reference (see Fig. 6).

Nevertheless, the character of the spin dependence of the extracted GDR parameters (see Sec. III C) is not significantly affected by the change of pairing reference, $r_0$ or $\gamma^{-1}$. This is because all the reactions studied are at approximately constant temperature, which implies constant $U$ in the level density Eqs. (1) and (2). Therefore, the level density changes very little as a function of spin, independent of the reference.

### 2. *The Pühlhofer approach and variations*

In the approach proposed by Pühlhofer,[25] originally used in the code CASCADE, the level density is defined separately in four regions. At the lowest excitation ($E_x \leq 5$ MeV), individual levels for the initial compound nucleus and for each daughter nucleus are counted. At higher energies, where the energies and spins of individual levels are unknown, the functional form of the level density proposed by Lang,[43] which is based on a Fermi gas model with equidistant levels, with parameters $a$ and $\Delta$, is applied. In the medium-energy range ($E_x \leq \sim 10$ MeV), the parameters $a$ and $\Delta$ are determined experimentally for each nucleus. At "high" energies ($E_x \geq \sim 20$ MeV), where shell and pairing effects are assumed to have vanished, smooth mass dependences for $a$ and $\Delta$ are assumed. The generally accepted values of $a_{\text{LDM}}=A/8$ MeV$^{-1}$, and $\Delta_{\text{LDM}}$ defined as the difference between experimental and liquid-drop binding energies calculated from the Myers droplet model mass formula[34] without shell and pairing corrections, are commonly used. In the transition region ($\sim 10$ MeV $\leq E_x \leq \sim 20$ MeV) between medium and high energies, a linear interpolation of $a$ and $\Delta$ is performed.

In the case of the Pühlhofer approach, the calculated level densities agree with experimental values at medium energies up to $E_x=8-10$ MeV for most of the nuclei (see Fig. 8), because the parameters $a$ and $\Delta$ (Refs. 32 and 44) used in the calculation have been extracted from fits to those level density data. At high energies, however, the magnitude of the level density determined by the parameters $a_{\text{LDM}}=A/8$ MeV$^{-1}$ and $\Delta_{\text{LDM}}$ calculated without the Wigner term[34] is too large for most of the nuclei. This results in an incorrect slope of the level density in the transition region ($E_x=10-20$ MeV), where the level density is interpolated between the medium and high energies. In such a case, the high-energy $\gamma$-ray spectrum for $\gamma$-decay populating states in the transition region is calculated incorrectly and fits often give unreasonable GDR parameters. We found this effect in the case of decay of the $^{63}$Cu* nucleus.[14] We also found that with some adjustment of parameters $a_{\text{LDM}}$ and $\Delta_{\text{LDM}}$ (which we call variations of the Pühlhofer approach[14]), we could reproduce the level density curves for nuclei near $A=63$ very

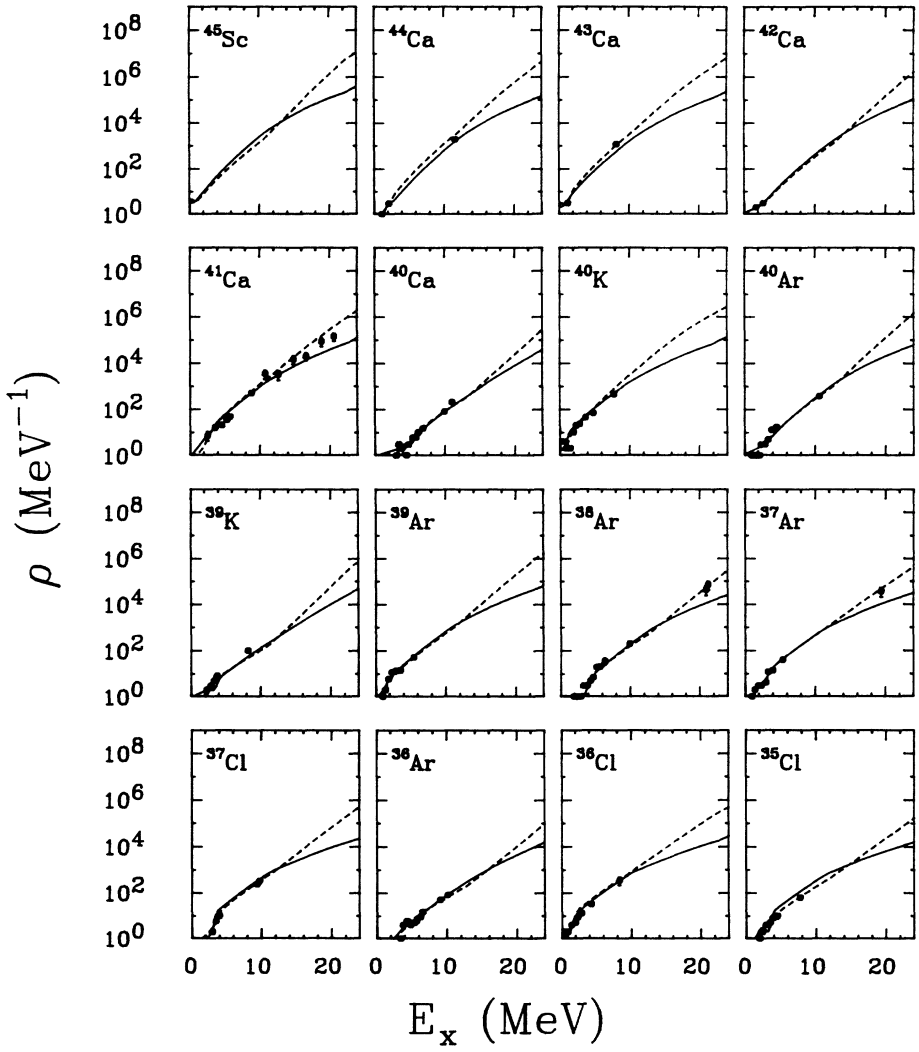


FIG. 8. Total level density curves for nuclei as in Fig. 2 but calculated using the Pühlhofer approach: dashes, $a_{\mathrm{LDM}} = A/8$ MeV$^{-1}$, and $\Delta_{\mathrm{LDM}}$ without the Wigner term; solid lines, $a_{\mathrm{LDM}} = A/10$ MeV$^{-1}$ and $\Delta_{\mathrm{LDM}}$ with the Wigner term.

well and extract reasonable GDR parameters.[14] We have observed a similar effect in our analyses of decays of $^{39}$K*, $^{42}$Ca*, and $^{45}$Sc* nuclei. Gamma-ray spectra from the decay of these nuclei at the initial excitation energy $E_{xi} \cong 40$ MeV can be fitted only if values smaller than $A/8$ MeV$^{-1}$ for the $a_{\mathrm{LDM}}$ parameter are used, especially for $^{39}$K* where values as low as $a_{\mathrm{LDM}} = A/10$ MeV$^{-1}$ and $\Delta_{\mathrm{LDM}}$ calculated with the Wigner term are required. Even with such a parametrization of the level density, however, the $\gamma$-ray spectrum shape for $^{40}$K* at $E_{xi} = 46.3$ MeV cannot be reproduced.

The observed inconsistency of the parameters $a_{\mathrm{LDM}}$ and $\Delta_{\mathrm{LDM}}$ required to reproduce the level density curves and the high-energy $\gamma$-ray spectra for neighboring nuclei seems to be connected with large differences in the ground-state shell effects in the mass range $A \cong 40$. The parameters $a$ and $\Delta$ defining the level density in the medium-energy range (3.5 MeV $\leq E_x \leq$ 11.5 MeV) have been extracted from the analysis[32,44] of the experimental level densities at energies up to 8–10 MeV. In this parametrization, the shell effects are included not only in the parameter $\Delta$ but also in the parameter $a$, which results in a significant variation in $a$ values for similar mass nuclei. The biggest difference occurs between $^{39}$K, for which $a = A/12.2$ MeV$^{-1}$ and $^{40}$K, with $a = A/7.2$ MeV$^{-1}$. It is then impossible to find, for all nuclei near $A \cong 40$, one constant value defining the parameter $a_{\mathrm{LDM}} = A/\mathrm{const}$ MeV$^{-1}$ which, together, with some realistic $\Delta_{\mathrm{LDM}}$, will determine the level density with a sensible slope in the transition region where the linear interpolation of $a$ and $\Delta$ between the medium- and high-energy range is performed.

Figure 8 shows the total level density curves for some of nuclei important in the decay of $^{39}$K,*, $^{40}$K*, $^{42}$Ca*, and $^{45}$Sc* compound nuclei. The dashed curves were obtained using the Pühlhofer approach with $a_{\mathrm{LDM}} = A/8$ MeV$^{-1}$ and $\Delta_{\mathrm{LDM}}$ calculated without the Wigner term, while the solid lines correspond to $a_{\mathrm{LDM}} = A/10$ MeV$^{-1}$ and $\Delta_{\mathrm{LDM}}$ including the Wigner term. For comparison, the experimental values of the level density taken from

TABLE III. Reaction parameters and fitted GDR parameters for the compound nuclear decays studied.

| Compound nucleus | $E_{xi}$ (MeV) | $I_f$ ($\hbar$) | $E_{\rm rot}$ (MeV) | $E_{xf}$ (MeV) | $T_f$ (MeV) | $S$ | $E_D$ (MeV) | $\Gamma$ (MeV) |
|---|---|---|---|---|---|---|---|---|
| $^{39}$K | 60.0 | 16.0 | 18.7 | 13.9 | 1.69 | 0.86±0.06 | 17.0±0.1 | 13.4±0.4 |
| | 50.0 | 13.0 | 12.5 | 14.3 | 1.71 | 0.77±0.05 | 16.8±0.1 | 11.6±0.4 |
| | 40.0 | 8.0 | 5.0 | 14.9 | 1.75 | 0.89±0.11 | 16.4±0.1 | 10.5±0.3 |
| $^{40}$K | 46.3 | 9.5 | 6.6 | 17.8 | 1.88 | 1.33±0.09 | 17.2±0.1 | 12.1±0.4 |
| $^{42}$Ca | 50.2 | 12.5 | 10.3 | 16.7 | 1.78 | 1.17±0.08 | 17.1±0.1 | 11.9±0.3 |
| | 40.2 | 8.0 | 4.4 | 16.5 | 1.77 | 1.19±0.08 | 17.7±0.1 | 11.6±0.3 |
| $^{45}$Sc | 66.6 | 18.5 | 19.6 | 17.8 | 1.78 | 0.97±0.07 | 16.3±0.1 | 14.7±0.5 |
| | 60.0 | 16.0 | 14.8 | 17.7 | 1.77 | 0.87±0.06 | 16.1±0.1 | 12.4±0.4 |
| | 50.0 | 13.0 | 9.9 | 16.8 | 1.73 | 0.76±0.05 | 16.1±0.1 | 12.1±0.4 |
| | 42.0 | 8.0 | 3.9 | 16.1 | 1.69 | 0.75±0.05 | 17.0±0.1 | 11.6±0.3 |

Beckerman[33] and Dilg *et al.*[32] are also presented in Fig. 8. Even though the dashed curves agree reasonably well with the level density data, the slope discontinuities present in several nuclei such as $^{39}$K lead to physically unreasonable GDR parameters at some bombarding energies.

Finally, we conclude that with the Pühlhofer approach we are not able to reproduce the level densities for all nuclei of interest in a consistent way, and which will result in good fits for all measured $\gamma$-ray spectra.

### C. GDR parameters

All measured $\gamma$-ray spectra were fitted using an isospin-dependent version of the code CASCADE with the level density calculated in the Reisdorf approach as discussed above, and a one-component GDR strength function. Final values of the mean GDR energy, width, and strength (in units of the classical dipole sum rule) extracted from least-squares fits (with the level density parameters $\gamma^{-1}=18.5$ MeV, $r_0=1.10$ fm and with the odd-$A$ pairing reference) are given in Table III. Errors in the GDR parameters include only statistics, except for the strength, which includes the absolute normalization uncertainty of 7–12%. Systematic errors are connected mainly with the uncertainty in the level density discussed in Sec. III B 1 and are estimated to be $\Delta S \cong \pm 15\%$, $\Delta E \cong \pm 0.5$ MeV, and $\Delta\Gamma \cong \pm 1$ MeV. These errors are due primarily to the uncertainty in the pairing reference; they also include contributions from estimated uncertainties in $r_0$ ($\pm 0.02$ fm) and $\gamma^{-1}$ ($\pm 6$ MeV). However, none of these uncertainties apply to the GDR parameter differences as a function of spin for a given reaction.

Also presented in Table III are the final energy $E_{xf}$ above the yrast line, the final average spin $I_f$ and effective temperature $T_f$ for each case calculated as in Ref. 14. The final energy $E_{xf}$ above the yrast line is defined as $E_{xf}=E_x-E_{\rm rot}-E_D$, where $E_x$ is the excitation energy of the decaying nucleus averaged over the initial compound nucleus and all daughter nuclei that contribute to the $\gamma$ decay with $E_\gamma \cong E_D$. The yrast energy calculated for the average final spin $I_f$ is $E_{\rm rot}=I_f(I_f+1)/\theta$, where the rigid-body moment of inertia $\theta$ is calculated with $r_{0\rm LDM}=1.30$ fm. The effective temperature was estimated as $T_f^2=E_{xf}/a$, where the level density parameter $a=A/8$ MeV$^{-1}$ was used.

In attempting to understand the properties of the GDR at high excitation energy, it is very useful to be able to compare with the properties of the GDR built on the ground state. The shape of the GDR built on the ground states of $^{39}$K, $^{42}$Ca, and $^{45}$Sc has been measured in photoneutron reactions (see Refs. 45–47, respectively) and the observed broadening of the $(\gamma,n)$ excitation curve was explained mainly by the (unresolved) isospin splitting of the GDR into two components, characterized by $T_<=T_3$ and $T_>=T_3+1$. For our purpose, we wish to know the properties of the $T_<$ component since only this component is formed in heavy-ion collisions. For the $^{42}$Ca nucleus[48,49] and the $^{45}$Sc nucleus[50,51] $T_<$ and $T_>$ components have also been observed in $(\gamma,p)$ excitation curves. For $^{42}$Ca (Ref. 48) and $^{45}$Sc (Ref. 47) a deformation splitting was also considered. The mean GDR energies estimated for $^{39}$K, $^{42}$Ca, and $^{45}$Sc are presented in Table IV. There are no available experimental data from photoproton or photoneutron reactions for $^{40}$K, so we es-

TABLE IV. Characteristics of the ground-state GDR isospin splitting for the nuclei of interest (see text).

| Nucleus | $T_3$ | $E_{\rm mean}$ (MeV) | $\Delta E$ (MeV) | $S_>/S_<$ | $E_<$ (MeV) |
|---|---|---|---|---|---|
| $^{39}$K | 1/2 | ~20 | 2.31 | 1.65 | ~18.6 |
| $^{40}$K | 1 | 19.7 | 3.0 | 0.77 | 18.4 |
| $^{42}$Ca | 1 | 20.0 | 2.86 | 0.78 | 18.7 |
| $^{45}$Sc | 3/2 | 19.0 | 3.33 | 0.49 | 17.9 |

timated the mean GDR energy for that nucleus based on $^{40}$Ca data.[52–54] The magnitude $\Delta E$ of the isospin splitting[55] (which is related to the nuclear symmetry energy), the calculated strength ratios[56] $S_>/S_<$ due to isospin splitting, and the estimated energies $E_<$ of the $T_<$ component of the GDR are presented in Table IV for the nuclei of interest. The width of the $T_<$ component of the ground-state GDR is difficult to estimate because the splitting is not resolved; however, the value $\Gamma_{g.s.} \cong 5$ MeV seems to be reasonable for these nuclei. The fraction of the classical dipole sum rule exhausted by the GDR built on the ground state has been estimated by taking into account both the $(\gamma,n)$ and $(\gamma,p)$ cross sections, with the result $S_{g.s.} \cong 0.85$ and 0.90 for $^{42}$Ca and $^{45}$Sc, respectively.

Although the effective temperatures in the present experiments are nearly constant (in the range of 1.7–1.8 MeV for most cases), the spins vary substantially, so that the results provide direct information on the spin dependence of the GDR in hot nuclei at constant temperature. This simplification of constant temperature is particularly important, as mentioned earlier, since the GDR width and shape are known to be strongly influenced by temperature as well as spin. The uncertainty in the average spin $I_f$ is due mainly to the determination of the grazing angular momentum $l_0$ in the entrance channel (see Sec. II A) and is small ($\cong 1\hbar$) based on a comparison of calculated and measured $\gamma$-ray spectra for $E_\gamma < 8$ MeV, assuming the strong absorption model with the transmission coefficient approximated by a Fermi distribution with diffuseness of 2 fm for the initial spin distribution. The resulting temperature uncertainty is of order 0.1 MeV. The uncertainties in the final spin and temperature are not sensitive to the choice of the reference in the level density calculations if the best parameters $r_0$ and $\gamma^{-1}$ are used in each case. The GDR parameters plotted as a function of the final average spin $I_f$ are shown in Fig. 9.

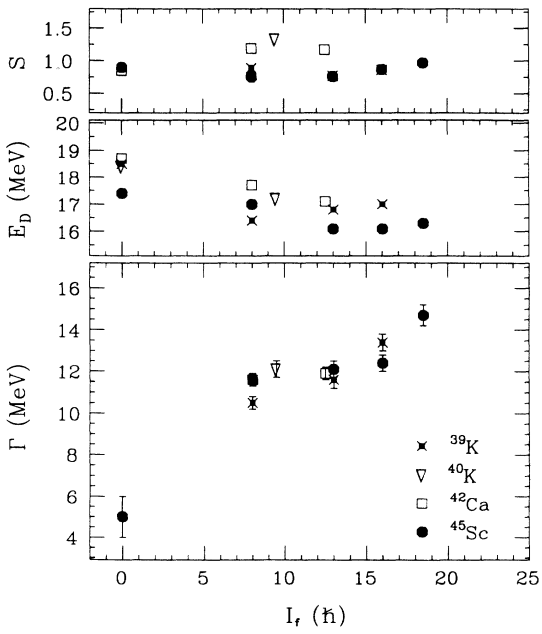


FIG. 9. The extracted GDR parameters as a function of final average spin. Ground-state GDR values are taken from Refs. 45–54 as described in the text.

For a given initial compound nucleus, the extracted GDR energies show some spin dependence. For the $^{45}$Sc* and $^{42}$Ca* compound nuclei, the GDR energy $E_D$ drops by 0.7 and 0.6 MeV respectively, while for $^{39}$K* it increases by 0.6 MeV. In all cases, the character of this spin dependence is not affected by a change of the pairing reference or the level density parameters $\gamma^{-1}$ and $r_0$, due mainly to the fact that the data all correspond to nearly the same temperature. The uncertainty in these energy shifts is estimated to be $\cong \pm 0.14$ MeV and is dominated by the statistical uncertainties. We made a further investigation to see if these shifts might be affected by an error in the shell correction, and again we found no significant dependence (specifically, for $^{45}$Sc* a change in $\delta U$ of 0.5 MeV changed the shift in $E_D$ with spin by 0.02 MeV).

In our previous study[14] of decays of $^{63}$Cu, no evidence for spin dependence of the GDR energy was found. In a study reported by Schwalm *et al.*,[22] the GDR energy in Er isotopes decreased with increasing spin from 5 to 50$\hbar$. In the recent experiment by Thirolf *et al.*[57] at the Darmstadt-Heidelberg crystal ball, similar effects have been observed. Also, Bruce *et al.*[58] have reported a shift in the $\gamma$-ray strength for $^{156}$Dy and $^{172}$Yb as a function of spin varying from 18 to 40$\hbar$, which could be interpreted as a reduction in the GDR energy or, alternatively, in terms of a shape transition between prolate and oblate shapes.

The fitted energies $E_D$ in Table II are consistently low compared to the $E_<$ estimates for the ground-state GDR given in Table IV. In fact, the discrepancy between the average value of $E_D$ and the corresponding $E_<$ estimate for each of the four nuclei is nearly the same, $\cong 1.5$ MeV, and is a factor of 3 larger than our estimated uncertainty in $E_D$ of $\pm 0.5$ MeV given earlier. We know of no explanation for these differences. They are clearly outside the uncertainties in our estimates of the mean energy for the ground-state GDR. An explanation in terms of increased isospin splitting would require twice the normal symmetry energy, which seems unreasonable. If decays to $T_>$ final states are significant in the present reactions, then the extracted $E_D$ values would be expected to be lower than the $E_<$ estimates, since the isospin splitting is greater for a GDR built on a $T_>$ state; however, we checked this effect and found it to be negligible. Isospin mixing, if important, would make this discrepancy even larger.

The GDR width increases smoothly with increasing final spin. The character of this dependence is similar for all the nuclei studied. It is also independent of the choice of the pairing reference. Even calculations using the Reisdorf parameter values ($r_0 = 1.153$ fm, $\gamma^{-1} = 18.5$ MeV) for the level density give the same rapid increase of the GDR width with spin. The main difference in the shape of the GDR strength function for these nuclei compared to the previously studied $^{63}$Cu* decays[14] is that in these lighter nuclei the GDR observed at the same spin and temperature is 2–5 MeV broader. However, if one

extrapolates the GDR widths in Fig. 9 to zero spin, one finds $\Gamma \cong 10$ MeV, which is similar to the value $\Gamma \cong 9$ MeV found for $^{63}Cu^*$ decays at similar temperature and low spin (see Fig. 12 of Ref. 14). Thus, the difference is that the GDR width increases more rapidly with spin in the present cases than it does in $^{63}Cu^*$. This is to be expected since, for a given spin, the rotational frequency in these light nuclei is about twice that of $^{63}Cu^*$. Hence, one expects larger spin-induced deformations, and, as a result, a larger GDR strength function width due to the deformation splitting in these lighter nuclei. Nevertheless, all of the present data are reasonably well fitted with a one-component GDR. This suggests that for these $^{39}K$, $^{40}K$, $^{42}Ca$, and $^{45}Sc$ nuclei at finite temperature $T \cong 1.7-1.8$ MeV the ensemble of excited nuclear states available in the process of thermal fluctuations (which are in large part responsible for the GDR width[59]) contains a broad distribution of deformations and the thermal averaging over this distribution washes out the GDR structure leaving only a very large width. The experimental proof that spin-induced deformation splitting plays an essential role in determining the shape of the GDR is presented in the discussion of angular distribution results in Sec. III D below.

The question arises as to whether the very broad GDR strength functions deduced in the present studies may be distorted by contamination from high-energy $\gamma$ rays produced in reactions other than fusion evaporation. It has been observed in previous studies of $^{12}C$ (Ref. 28), $^{15}N$ (Ref. 29), and $^{18}O$ (Refs. 30 and 31) induced reactions on $^{27}Al$ that the measured fusion-evaporation cross section $\sigma_{ER}$ exhausts more than 75% of the total reaction cross section $\sigma_R$ for the highest projectile energies presently studied and more than 80% for lower projectile energies. The difference between $\sigma_R$ and $\sigma_{ER}$ is attributed to the deep-inelastic cross section $\sigma_{\rm DIC}$ and quasielastic cross section $\sigma_{\rm QB}$. The quasielastic process does not produce high-energy $\gamma$ rays. For $^{12}C+^{27}Al$ at 62 MeV[60] and $^{16}O+^{27}Al$ at 72.5 MeV,[61] the contribution of $\sigma_{\rm DIC}$ to the reaction cross section was found to be less than 4%. In order to estimate the effect of deep-inelastic scattering on the high-energy $\gamma$-ray spectrum, the $\gamma$-ray spectrum following the decay of deep-inelastic fragments produced in $^{12}C+^{27}Al$ at 62.7 MeV and $^{18}O+^{27}Al$ at 72.5 MeV were calculated using the CASCADE code. We assumed the product masses to be the same as in the entrance channel and that the intrinsic energy of the two-body system (total energy minus Coulomb repulsion energy for two touching spheres) divides equally between light and heavy fragments. For both reactions the resulting $\gamma$-ray spectrum is of the order of 1% or less of the statistical spectrum at energies $E_\gamma = 8$ MeV and of the order of 0.2% or less for energies $E_\gamma \geq 15$ MeV, and hence the extracted GDR parameters are completely insensitive to this effect. Similar results are obtained for a fission-like process producing two equal mass fragments.

The only other known process which might cause trouble is the heavy-ion bremsstrahlung; however, at these low bombarding energies $E/A \leq 6$ MeV/nucleon, there is no evidence from other studies for this process. Indeed, there is evidence from other studies for pure statistical emission at these energies (e.g., Refs. 10 and 14). Also, the measured angular distributions (see Sec. III D) are consistent with $a_1 = 0$ up to the highest $\gamma$-ray energies, in contrast to the positive $a_1$ expected for bremsstrahlung.[62]

### D. Angular distributions

We measured angular distributions of $\gamma$ rays from the decay of $^{39}K^*$ at initial excitation energy $E_{\rm xi} = 60.0$ MeV and $^{45}Sc^*$ at $E_{\rm xi} = 50.0$ and 66.6 MeV. The measured cross section at each angle has been transformed from the laboratory to center-of-mass frame (c.m.) by accounting for Doppler shifts in $\gamma$-ray energy:

$$E_{\gamma,\rm c.m.} = \gamma[1-\beta\cos(\theta_{\rm lab})]E_{\gamma,\rm lab}$$

and converting the laboratory cross section and angle into the center-of-mass system according to the formulas

$$\tan(\theta_{\rm c.m.}) = \frac{\sin(\theta_{\rm lab})}{\gamma[\cos(\theta_{\rm lab})-\beta]} ,$$

$$\frac{d^2\sigma_{\rm c.m.}}{d\Omega_{\rm c.m.}dE_{\gamma,\rm c.m.}} = \frac{\sin^2(\theta_{\rm lab})}{\sin^2(\theta_{\rm c.m.})}\frac{1}{\gamma[1-\beta\cos(\theta_{\rm lab})]} \times \frac{d^2\sigma_{\rm lab}}{d\Omega_{\rm lab}dE_{\gamma,\rm lab}} ,$$

where $\beta = v_{\rm c.m.}/c$, $v_{\rm c.m.}$ is the velocity of the center-of-mass frame and $\gamma = (1-\beta^2)^{-1/2}$. The center-of-mass cross section as a function of angle and $\gamma$-ray energy was fitted with a Legendre polynomial expansion of the form

$$\frac{d^2\sigma_{\rm c.m.}(\theta_{\rm c.m.},E_{\gamma,\rm c.m.})}{d\Omega_{\rm c.m.}dE_{\gamma,\rm c.m.}} = A_0(E_{\gamma,\rm c.m.})[1+a_1(E_{\gamma,\rm c.m.})P_1(\cos\theta_{\rm c.m.})+a_2(E_{\gamma,\rm c.m.})P_2(\cos\theta_{\rm c.m.})] .$$

In Fig. 10 the fitted parameters $a_1$ and $a_2$ are shown as a function of $\gamma$-ray energy $E_\gamma$ (here and below, $E_\gamma$, $\theta$, $a_1$, and $a_2$ refer to c.m. quantities) for the three cases studied. For all three cases, the coefficient $a_1$ is consistent with zero for $E_\gamma \geq 10$ MeV, within experimental uncertainty. This behavior is predicted for statistical emission of $\gamma$ rays, which involves averaging over many initial states of the thermally equilibrated compound system. A zero $a_1$ coefficient, although it is not sufficient to prove a statistical mechanism for the reactions studied, does imply that any enhancement from a nonstatistical process like that observed at high $\gamma$-ray energies for $^3He$, $^4He$ (Refs. 8 and 10) and $^6Li$ (Ref. 14) projectiles is negligible. It also weighs against a bremsstrahlung contribution due

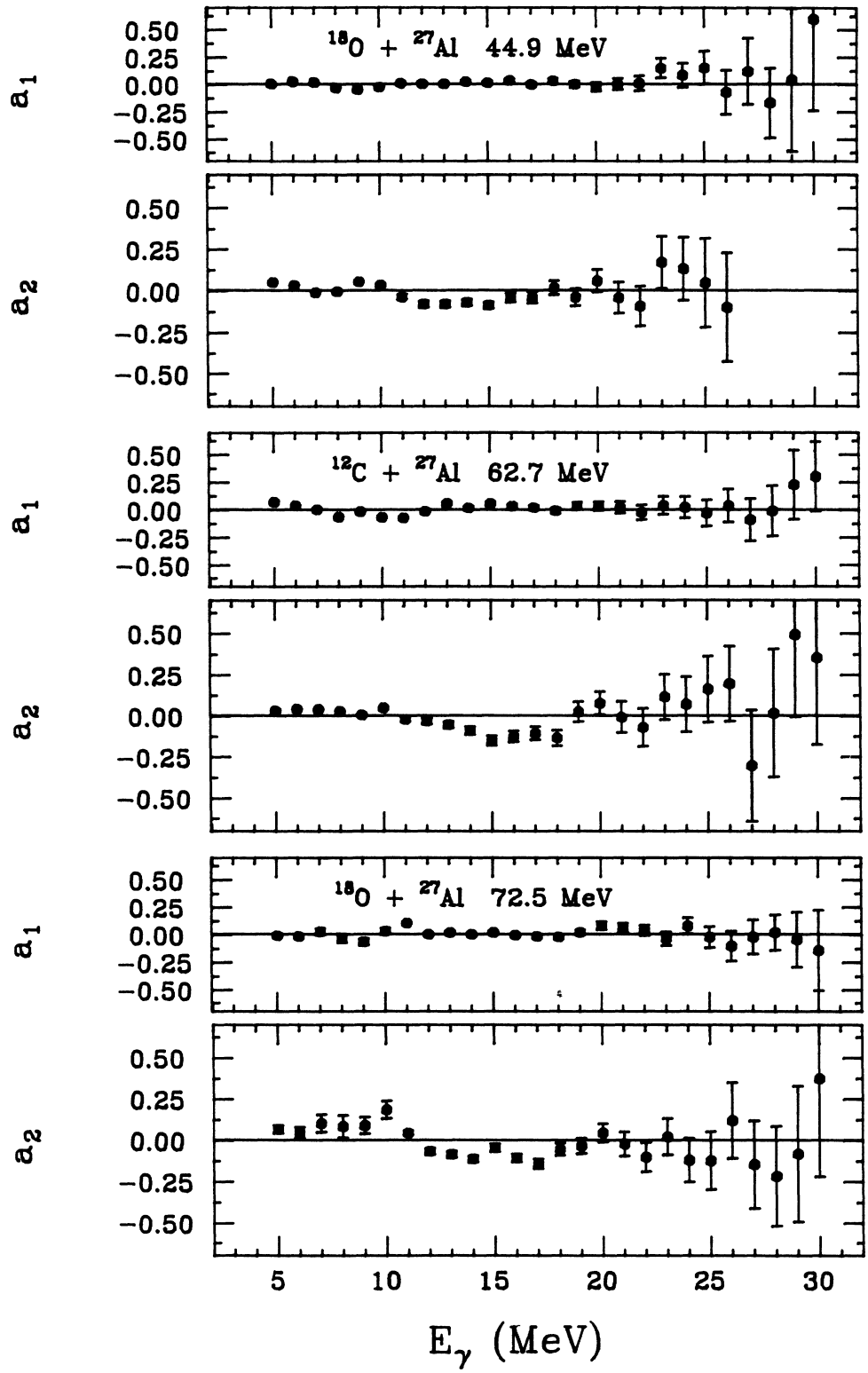


FIG. 10. Angular distribution coefficients $a_1$ and $a_2$ for reactions $^{12}C+^{27}Al \rightarrow ^{39}K^*$ at $E_{lab}=62.7$ MeV and $^{18}O+^{27}Al \rightarrow ^{45}Sc^*$ at $E_{lab}=44.9$ and 72.5 MeV as a function of $\gamma$-ray energy.

to a nucleon-nucleon collision mechanism, which should be somewhat forward peaked in the c.m. frame.

The $a_2$ coefficient above $E_\gamma=10$ MeV has a small negative value ($|a_2| \leq 0.15$) and it is zero or slightly positive for $E_\gamma \geq 20$ MeV. At low $\gamma$-ray energies (4–8 MeV), the measured $\gamma$-ray spectra at the highest projectile energies and especially at forward angles show some structure visible as small bumps above the smooth statistical part

of the spectrum, and the $a_1$ coefficient is positive. The energies of these bumps agree with lines produced when the same projectile bombards natural carbon and oxygen targets, but their relative strengths are different, which makes any subtraction of this "impurity" impossible. The yield of these "impurity" bumps is also much larger than expected, based on the estimated amount of light impurities in our aluminum targets (Sec. II). Therefore, we infer that these bumps are due to $\gamma$ decay of projectile-like reaction products which are moving with an average velocity $\beta/\beta_{\text{c.m.}}$ in the beam direction. Thus, since the low-energy part of the spectra has some contamination due to nonstatistical process, we discuss $a_2$ coefficients for these two cases only above 10 MeV, where we are confident that only statistical decay is taking place.

### E. Interpretation of angular distributions

The observed dependence of $a_2$ on $E_\gamma$ in the GDR region $E_\gamma > 10$ MeV is qualitatively similar for all three reactions shown in Fig. 10; namely, small negative values with a magnitude $|a_2| \leq 0.15$ on the low-energy side of the GDR, $E_\gamma < E_D$, and zero or somewhat positive values for $E_\gamma > E_D$. These anisotropies provide model-independent evidence for a preferred deformation of the rotating, decaying nucleus (see, e.g., Refs. 10 and 63). A dispersion curve for $a_2$ vs $E_\gamma$, centered on $E_\gamma = E_D$, is just what is expected for deformation splitting of the GDR, and the sign of the curve—negative $a_2$ values for $E_\gamma < E_D$—indicates that the short axis of the deformed nuclear shape is preferentially aligned in the spin direction, and rules out the other possibility, namely that the shape is preferentially aligned with its long axis in the direction of the spin. If the nuclear shape is axially symmetric, then the allowed orientations correspond to either oblate noncollective or prolate collective rotation, while oblate collective and prolate noncollective rotation are ruled out. More generally, the nuclear shape may be triaxial; then the allowed orientations correspond to $-30° \leq \gamma \leq 60°$ where $\gamma$ is the usual quadrupole shape parameter with prolate collective rotation and oblate noncollective rotation corresponding to the $\gamma = 0°$ and 60°, respectively.

The sign of the dispersion curve for $a_2$ vs $E_\gamma$ does not allow one to distinguish between the interesting possibilities of oblate noncollective and prolate collective rotation. The detailed shape of the curve might allow such a distinction if $a_2$ could be determined with good precision for $E_\gamma > E_D$, where different magnitudes are expected for these two possibilities. Unfortunately, the statistics are poor in this region (this is generally true in statistical decay studies, due to the exponentially dropping spectrum shape) and do not allow such a distinction. However, at these high temperatures $T_f \cong 1.7$–$1.8$ MeV, shell effects should be mostly washed out, and the nuclear shape should be well approximated by that of a rotating liquid drop. Thus oblate (noncollective) deformations which grow with spin are expected.[18] This may be quantified by the liquid-drop calculations of Cohen, Plasil, and Swiatecki.[64] They predict for $^{45}$Sc at spin $I = 18.5\hbar$ a deformation $\Delta R/R \cong 0.18$ ($\cong\beta$, where $\beta$ and $\gamma$ are the usual quadrupole shape parameters). Since we expect $\Delta E/E_D \cong \Delta R/R$, this leads to an expected deformation splitting $\Delta E \cong 3$ MeV, which is comparable to the observed spin broadening shown in Fig. 9.

In order to make a quantitative interpretation of the measured angular anisotropies in terms of deformation, it is necessary to account for the broadening of the GDR due to thermal fluctuations in the deformation. We have performed deformation averaging calculations (see also Ref. 65) along the lines of Gallardo *et al.*[59,66] using the metric $\beta d\beta d\gamma$. We assumed a parabolic shape for the free energy of the form

$$F = c[(x-x_0)^2 + (y-y_0)^2] ,$$

where $x = \beta\sin\gamma$, $y = \beta\cos\gamma$, and where the oblate minimum $(x_0, y_0)$ corresponds to $\gamma_0 = 60°$ with $\beta_0$ adjusted to fit the data. The curvature $c$ was chosen to be 30 MeV, a value that is approximately correct for nuclei at these temperatures.[67] The calculation was performed for a rotating harmonic-oscillator potential, assuming a GDR splitting (at zero spin) proportional to $1/R_j$, where the $R_j$ are the principal axes of the deformed shape. The

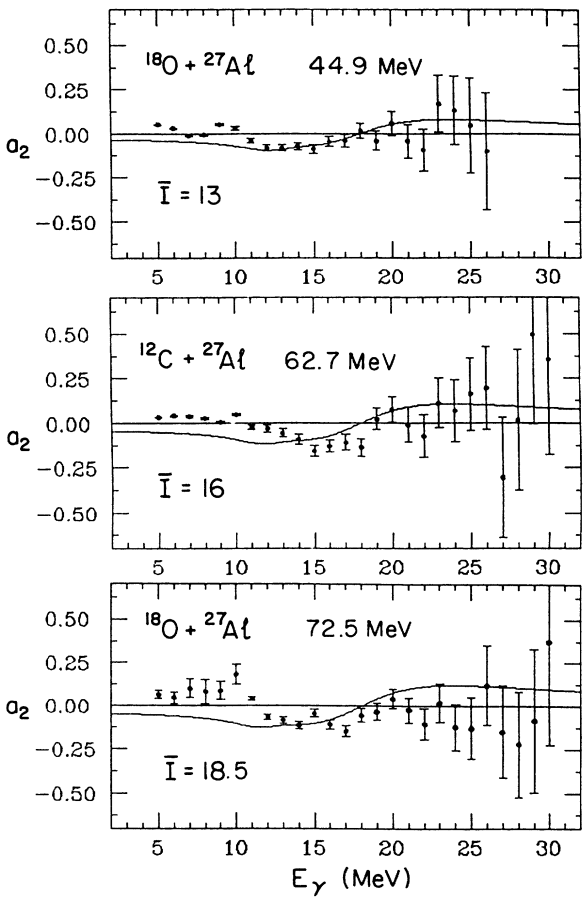


FIG. 11. Solid dots: measured $a_2$ coefficients (in the center of mass) as in Fig. 10. The curves are calculations (see text) with oblate deformation $\beta_0 = 0.10$ (top), 0.13 (middle), and 0.15 (bottom). The mean final state spin $I$ (in units of $\hbar$) are indicated on the figure.

intrinsic GDR width (spreading width) was assumed to vary as $\Gamma_j = \Gamma_0 (E_j / E_0)^{1.9}$ (Ref. 68) where $\Gamma_0 = 5$ MeV and $E_0$ = mean GDR energy (a similar relation describes well the width of the split GDR components in the rare-earth and actinide mass regions). The calculated anisotropies depend strongly on $\beta_0$, but weakly on $T$ (hence also $c$) and on $I$. A comparison of measured and calculated $a_2$ coefficients is shown in Fig. 11. The calculations, which are for a fixed equilibrium deformation and alignment, apply to the high-energy part of the spectrum with $E_\gamma \geq 11-12$ MeV. For lower $E_\gamma$, the increasing importance of daughter contributions from decays at lower spin (and weaker alignment) and energy, hence smaller deformation, should tend to drive the $a_2$ towards, zero, as is observed. The three different data sets are consistent with $\beta_0$ in the range 0.10–0.15, as shown in Fig. 11. These deformation averaging calculations fail by about 30% to reproduce the large widths observed for the strength distributions; hence the oblate deformation values deduced by comparing the calculated curves with experiment should be regarded as lower limits. Nevertheless, these results are in reasonable agreement with the liquid-drop expectations discussed above.

## IV. SUMMARY AND CONCLUSION

The purpose of the present study was to examine the spin dependence of the GDR strength function in equilibrated hot nuclei with mass $A \cong 40$ at constant effective temperature. We produced $^{39}$K*, $^{40}$K*, $^{42}$Ca*, and $^{45}$Sc* compound nuclei at nearly constant temperature $T_f = 1.7-1.8$ MeV and average final spin varying from 8 to 18.5$\hbar$.

In order to obtain statistical model calculations consistent with all of the measured spectra, it was necessary to improve the nuclear level density description beyond that commonly used. We found a good description of the level density using the formulation given by Reisdorf,[24] with a properly adjusted radius parameter $r_0$ suitable for these light nuclei, and with pairing energies determined with an odd-$A$ mass reference. It accounts for level densities at neutron threshold in an average manner, and includes the damping of shell effects with increasing energy. It also provides a reasonable model basis for determining the $a$ parameter, as opposed to the commonly used and somewhat arbitrary value $a = A/8$ MeV$^{-1}$. This formulation is to be preferred over other approaches, particularly for problems in which the level density at excitation energies $E_x \leq 40$ MeV, where the damping of shell effects is important, plays a role. We found an apparent spin dependence in the GDR energy for $^{39}$K (a decrease of $\Delta E = 0.6$ MeV with increasing spin) and $^{42}$Ca and $^{45}$Sc (an increase of 0.6 and 0.7 MeV, respectively), unaffected by uncertainties in level density parameters $r_0$, $\gamma^{-1}$, pairing reference, and $\delta U$. In addition, the mean GDR energies $E_D$ for each nucleus are found to be systematically low by $\cong 1.5$ MeV compared with the $E_<$ estimates for the ground-state GDR.

The GDR width (FWHM of the strength distribution) was found to vary smoothly from 11 to 15 MeV over the spin range 8–18.5$\hbar$. These broad widths may be compared to $\Gamma \cong 5$ MeV estimated for the $T_<$ component of the ground-state GDR. The width extrapolated to zero spin is $\cong 10$ MeV, comparable to the $\cong 9$ MeV value found at low spin and similar temperature for the decay of $^{63}$Cu*. The spin broadening at constant temperature is comparable to that expected for oblate deformation splitting of the GDR with a deformation given by the rotating liquid-drop model. This splitting is unresolved in the GDR strength function presumably because it is obscured by the additional broadening due to thermal fluctuations.

The observed spin dependences of all the GDR parameters $S$, $E_D$, and $\Gamma$, are insensitive to level density parameter uncertainties, since the different cases are at approximately constant temperature (constant $U$). Thus, not only is constant temperature an important condition which allows us to study the pure spin dependence of the GDR parameters, it also considerably reduces the sensitivity of the deduced values to the most uncertain aspect of the statistical model calculations, namely the level density.

Measured $\gamma$-ray angular distributions were found to be symmetric about $\theta = 90°$ in the center of mass, confirming the statistical nature of these reactions. The observed $a_2$ coefficients require a preferred deformation different from zero, with either an oblate shape rotating noncollectively or a prolate shape rotating collectively. Reasonable agreement is obtained between measured and calculated angular distributions in which the calculations include the effects of deformation averaging, and for which the preferred deformations are oblate and comparable in magnitude ($\beta \leq 0.2$) to values expected from a rotating liquid-drop model. More detailed calculations together with new data at higher bombarding energies (higher spins) will be presented in a forthcoming publication.

## ACKNOWLEDGMENTS

We thank K. Weber for his contributions to the deformation averaging calculations. One of us (M.K.-H) would like to thank the members of the University of Washington Nuclear Physics Laboratory for their generous hospitality. Financial support from the U.S. Department of Energy and the Polish Ministry of National Education (under Project CPBP 01.06) is gratefully acknowledged.

*Present address: Triangle Universities Nuclear Laboratory, Duke University, Durham, NC 27706.

[1] J. O. Newton, B. Herskind, R. M. Diamond, E. L. Dines, J. E. Draper, K. H. Lindenberger, C. Schuck, S. Shih, and F. S. Stephens, Phys. Lett. **46**, 1383 (1981).

[2] J. E. Draper, J. O. Newton, L. G. Sobotka, H. Lindenberger, G. J. Wozniak, L. G. Moretto, F. S. Stephens, R. M. Diamond, and R. J. McDonald, Phys. Rev. Lett. **49**, 434 (1982).

[3]A. M. Sandorfi, J. Barrette, M. T. Collins, D. H. Hoffmann, A. J. Kreiner, D. Branford, S. G. Steadman, and J. Wiggins, Phys. Lett. **130B**, 19 (1983).
[4]W. Hennerici, V. Metag, H. J. Hennrich, R. Repnow, W. Wahl, D. Habs, K. Helmer, U. V. Helmolt, H. W. Heyng, B. Kolb, D. Pelte, D. Schwalm, R. S. Simon, and R. Albrecht, Nucl. Phys. **A396**, 329c (1983).
[5]E. F. Garman, K. A. Snover, S. H. Chew, S. K. B. Hesmondhalgh, W. N. Catford, and P. M. Walker, Phys. Rev. C **28**, 2554 (1983).
[6]J. J. Gaardhøje, O. Andersen, R. M. Diamond, C. Ellegaard, L. Grodzins, B. Herskind, Z. Sujkowski, and P. M. Walker, Phys. Lett. **139B**, 273 (1984).
[7]J. J. Gaardhøje, C. Ellegaard, and B. Herskind, Phys. Rev. Lett. **53**, 148 (1984).
[8]K. A. Snover, Comment Nucl. Part. Phys. **12**, 243 (1984); J. Phys. (Paris) Colloq **45**, C4-337 (1984); *Capture Gamma-Ray Spectroscopy and Related Topics (Holiday Inn, World's Fair, Knoxville, Tennessee),* Proceedings of the Fifth International Symposium on Capture Gamma-Ray Spectroscopy and Related Topics, AIP Conf. Proc. No. 125, edited by S. Raman (AIP, New York, 1984), p. 660.
[9]C. A. Gossett, K. A. Snover, J. A. Behr, G. Feldman, and J. L. Osborne, Phys. Rev. Lett. **54**, 1486 (1985).
[10]K. A. Snover, Annu. Rev. Nucl. Part. Sci. **36**, 545 (1986).
[11]J. J. Gaardhøje, C. Ellegaard, B. Herskind, R. M. Diamond, M. A. Deleplanque, G. Dines, A. O. Macchiavelli, and F. S. Stephens, Phys. Rev. Lett. **56**, 1783 (1986).
[12]M. N. Harakeh, D. H. Dowell, G. Feldman, E. F. Garman, R. Loveman, J. L. Osborne, and K. A. Snover, Phys. Lett. B **176**, 297 (1986).
[13]D. R. Chakrabarty, M. Thoennessen, N. Alamanos, P. Paul, and S. Sen, Phys. Rev. Lett. **58**, 1092 (1987).
[14]M. Kicińska-Habior, K. A. Snover, C. A. Gossett, J. A. Behr, G. Feldman, H. K. Glatzel, J. H. Gundlach, and E. F. Garman, Phys. Rev. C **36**, 612 (1987).
[15]A. Stolk, W. H. A. Hesselink, H. Rijneveld, A. Balanda, J. Penninga, and H. Verheul, Phys. Lett. B **200**, 13 (1988).
[16]S. Henss, A. Ruckelshausen, R. D. Fischer, W. Kuhn, V. Metag, and R. Novotny, R. V. F. Janssens, T. L. Khoo, D. Habs, D. Schwalm, D. Freeman, G. Duchene, B. Haas, F. Hass, S. Hlavac, and R. S. Simon, Phys. Rev. Lett. **60**, 11 (1988).
[17]W. Scholz and F. B. Malik, Phys. Rev. **153**, 1071 (1967); W. J. Childs, Phys. Rev. A **4**, 1767 (1971).
[18]S. Aberg and G. Leander, Nucl. Phys. **A332**, 365 (1979).
[19]G. Shanmugam and V. Devanathan, Phys. Scr. **24**, 17 (1981).
[20]G. Shanmugam and V. Devanathan, Phys. Scr. **25**, 607 (1982).
[21]K. Neergard, Phys. Lett. **110B**, 7 (1982).
[22]D. Schwalm, Ch. Ender, H. Groger, D. Habs, U. V. Helmolt, W. Hennerici, H. J. Hennerich, H. W. Heyng, W. Korten, R. Kroth, M. Music, J. Schrimer, B. Schwartz, W. Wahl, R. S. Simon, W. Kühn, V. Metag, and C. Broude, Max-Planck Institut für Kernphysik Report MPI H-1984-V35, 1984.
[23]C. A. Gossett, J. A. Behr, G. Feldman, J. H. Gundlach, and K. A. Snover, University of Washington, Nuclear Physics Laboratory Annual report, 1986, p. 14.
[24]W. Reisdorf, Z. Phys. A **300**, 227 (1981).
[25]F. Pühlhofer, Nucl. Phys. **A280**, 267 (1977).
[26]B. L. Berman and S. C. Fultz, Rev. Mod. Phys. **47**, 713 (1975).
[27]F. E. Bertrand, Annu. Rev. Nucl. Sci. **26**, 457 (1976).
[28]J. B. Natowitz, E. T. Chulick, and M. N. Namboodiri, Phys. Rev. C **6**, 2133 (1972).
[29]F. W. Prosser, Jr., R. A. Racca, K. Daneshvar, D. F. Geesaman, W. Henning, D. G. Kovar, K. E. Rehm, and S. L. Tabor, Phys. Rev. C **21**, 1819 (1980).
[30]Y. Eisen, I. Tserruya, Y. Eyal, Z. Fraenkel, and M. Hillman, Nucl. Phys. **A291**, 459 (1977).
[31]R. Rascher, W. F. J. Müller, and K. P. Lieb, Phys. Rev. C **20**, 1028 (1979).
[32]W. Dilg, W. Schantl, H. Vonach, and M. Uhl, Nucl. Phys. **A217**, 269 (1973).
[33]M. Beckerman, Nucl. Phys. **A278**, 333 (1977).
[34]W. D. Myers, *Droplet Model of Atomic Nuclei* (IFI/Plenum, New York, 1977).
[35]K. H. Schmidt, H. Delagrange, J. P. Dufour, N. Carjan, and A. Fleury, Z. Phys. A **308**, 215 (1982).
[36]W. D. Myers (private communication).
[37]D. Vermeulen, H. G. Clerc, C. C. Sahm, K. H. Schmidt, J. Keller, G. Munzenberg, and W. Reisdorf, Z. Phys. A **318**, 157 (1984); C. C. Sahm, H. G. Clerc, K. H. Schmidt, W. Reisdorf, P. Armbruster, F. P. Hesseberger, J. G. Keller, G. Munzenberg, and D. Vermeulen, Nucl. Phys. **A441**, 316 (1985).
[38]W. D. Myers, Nucl. Phys. **A204**, 465 (1973).
[39]H. de Vries, C. W. de Jager, and C. de Vries, At. Data Nucl. Data Tables **36**, 495 (1987).
[40]W. D. Myers, At. Data Nucl. Data Tales **17**, 411 (1976).
[41]J. Blocki, J. Randrup, W. J. Swiatecki, and C. F Tsang, Ann. Phys. **105**, 427 (1977).
[42]W. D. Myers and W. J. Swiatecki, Nucl. Phys. **A336**, 267 (1980).
[43]D. W. Lang, Nucl. Phys. **77**, 545 (1966).
[44]H. Vonach and M. Hille, Nucl. Phys. **A127**, 289 (1969).
[45]D. V. Webb, E. G. Muirhead, and B. M. Spicer, Nucl. Phys. **A171**, 324 (1971).
[46]Y. I. Assafiri and M. N. Thomson, Nucl. Phys. **A357**, 429 (1980).
[47]R. H. Sambell and B. M. Spicer, Nucl. Phys. **A205**, 139 (1973).
[48]E. M. Diener, J. F. Amann, P. Paul, and J. D. Vergados, Phys. Rev. C **7**, 705 (1973).
[49]R. E. Pywell, M. N. Thomson, K. Shoda, M. Sugawara, T. Saito, H, Tsubota, H. Miyase, J. Vegaki, T. Tamae, H. Ohashi, and T. Urano, Aust. J. Phys. **33**, 685 (1980).
[50]S. Oikawa and K. Shoda, Nucl. Phys. **A277**, 301 (1977).
[51]D. Ryckbosch, E. Van Camp, R. Van de Vyver, E. Kerkhove, P. Van Otten, P. Berkvens, and H. Ferdinande, Phys. Rev. C **26**, 448 (1982).
[52]I. Bergqvist, R. Zorro, A. Hakansson, A. Lindholm, L. Nilsson, N. Olsson, and A. Likar, Nucl. Phys. **A419**, 509 (1984).
[53]C.-P. Wu, J. E. E. Baglin, F. W. K. Firk, and T. W. Phillips, Phys. Lett. **29B**, 359 (1969).
[54]E. M. Diener, J. F. Amann, and P. Paul, Phys. Rev. C **7**, 695 (1973).
[55]R. O. Akyuz and S. Fallieros, Phys. Rev. Lett. **27**, 1016 (1971).
[56]S. Fallieros and B. Goulard, Nucl. Phys. **A147**, 593 (1970).
[57]P. Thirolf, D. Habs, D. Schwalm, R. D. Fisher, and V. Metag, Proceedings of the First Topical Meeting on Giant Resonance Excitation in Heavy-Ion Collisions, Legnaro, Italy, 1987 [Nucl. Phys. **A482**, 93c (1988)].
[58]A. M. Bruce, J. J. Gaardhøje, B. Herskind, R. Chapman, J. C. Lisle, F. Khazaie, and J. N. Mo, Phys. Lett. B **215**, 237 (1988).
[59]M. Gallardo, M. Diebel, T. Døssing, and R. A. Broglia, Nucl. Phys. A **443**, 415 (1985).
[60]Fen Enpu, Wang Qi, Zhu Yongtai, Yin Xu, Miao Hebin, Sun Shumin, Li Songlin, Wu Zhongli, and Fan Guoyin, in *Heavy-Ion Fusion Reactions,* Proceedings of the Tsukuba International Symposium, Tsukuba, Japan, 1984, edited by K. Furmo

and T. Kishimoto (World-Scientific, Singapore, 1985), p. 401.
[61]Zhu Yongtai, Shen Wenqing, Zhan Wenlong, Guo Zhongyan, Yen Shuzhi, Jin Genmin, Qiao Weimin, and Wu Enchiu, in *Heavy-Ion Fusion Reactions,* Proceedings of the Tsukuba International Symposium (Ref. 60), p. 403.
[62]V. Metag, Nucl. Phys. **A488**, 483c (1988).
[63]K. A. Snover, Nucl. Phys. **A482**, 13c (1988) (see Ref. 57).
[64]S. Cohen, F. Plasil, and W. J. Swiatecki, Ann. Phys. (N.Y.) **82**, 557 (1974).
[65]K A. Snover, *Contemporary Topics in Nuclear Structure Physics,* edited by R. F. Casten *et al.* (World-Scientific, Singapore, 1988), p. 251.
[66]M. Gallardo, F. J. Luis, and R. A. Broglia, Phys. Lett. **191**, 222 (1987).
[67]Y. Alhassid and B. Bush (private communication).
[68]K. A. Snover, in *The Response of Nuclei Under Extreme Conditions,* Proceedings of the 1986 Erice Summer School, edited by R. A. Broglia and G. F. Bertsch (Plenum, New York, 1988), p. 69.